Giant, 12, 2022, 100118

Full-length article

Searching for the simplest self-assembling dendron to study helical self-organization and supramolecular polymerization

Mihai Peterca [a], Dipankar Sahoo [a], Mohammad R. Imam [a,b], Qi Xiao [a], Virgil Percec [a,*]

[a] Roy & Diana Vagelos Laboratories, Department of Chemistry, University of Pennsylvania, 6323, Philadelphia, PA 19104, USA
[b] Mathematics and Natural Sciences Department, American University of Iraq, Sulaimani (AUIS), Sulaimani, Kurdistan Region 46001, Iraq

Keywords: **Helical, Self-organization, Supramolecular polymerization, First generation, Self-assembling dendron, Structural simplicity**

The first generation self-assembling dendron (4Bp-3,4)nG1CO$_2$CH$_3$ where Bp is biphenyl, n is an achiral linear, *n*-dodecyl, or branched chiral alkyl group, (*S*)-3,7-dimethyl-octyl (dm8*) undergoes helical self-organization in bulk state and in solution. The supramolecular columns assembled from this dendron are helical, regardless, if the alkyl groups on its periphery are achiral or chiral. This demonstrates self-organization of helical columns both from achiral and chiral dendrons and reveals that the role of the stereocenter is to select the helical sense of an already helical column. This very simple self-assembling dendron can be subjected to a large diversity of chemical modifications and functionalization, all expecting to maintain the helical function in bulk and in solution in the range of temperature of interest to investigate helical self-organization and supramolecular polymerization.

Introduction

There is an ideal list of fundamental requirements of self-assembling building blocks employed to study helical self-organization and supramolecular polymerization. This list includes: a reasonable range of temperatures in which the supramolecular assembly is stable both in bulk and in solution; access to the monomeric building block employed in the self-assembly process *via* a minimum number of simple and, if possible, quantitative reaction steps employing easily accessible starting materials; suitable UV, circular dichroism (CD), and NMR spectra both in self-assembled solution and in film state; shape persistence between the helical supramolecular structure from bulk state and the one generated in solution, and the elucidation of the supramolecular structure in bulk state, preferably by X-ray diffraction (XRD) experiments. Self-assembling dendrons and dendrimers represent some of the simplest building blocks employed to investigate helical self-organization and supramolecular polymerization. However, according to our knowledge very few self-assembling dendrons and dendrimers employed in helical self-organization and supramolecular polymerization experiments fulfill at least part of the requirements mentioned above. They are dendritic dipeptides whose detailed structure in bulk state and in solution as well as the role of all molecular parameters of the self-assembling building block including constitutional isomerism and all possible stereochemical permutations were elucidated [1–11]. The role of the molecular parameters on the water transport of the supramolecular helical channel self-assembled from the dendritic dipeptide, that acts as an Aquaporin transmembrane

* Corresponding author.
E-mail address: percec@sas.upenn.edu (V. Percec).
Received 25 August 2022; Received in revised form 6 September 2022; Accepted 7 September 2022

 https://doi.org/10.1016/j.giant.2022.100118

protein channel mimic, helped to pioneer the field of water membranes that exhibit even higher selectivity and rate of water transport than natural transmembrane protein channels [1,6,12–24]. Dendritic dipeptides were also used to address the fundamental question of why homochirality is demanded by biology [9,11]. However, in spite of the great utility of this self-assembled system its synthetic access is limited to laboratories with both excellent synthetic and structural analysis capabilities. The second self-assembling building block elaborated with the same level of precision as the dendritic dipeptides mentioned above is a family of hat-shaped self-assembling dendrimers [25]. The unique characteristic of this system is its ability to undergo chiral self-sorting or deracemization in crystal state. Most probably hat-shaped self-assembling dendrimers represent the first system exhibiting deracemization in crystal state. The third self-assembling system represents a group of carefully designed dendronized perylene bisimides that provide helical supramolecular polymerization followed by deracemization *via* a novel cogwheel mechanism [26–29]. However, these three classes of self-assembling dendrons and dendrimers represent a very small number of suitable and well characterized systems considering the large activity in the field of helical self-organization and supramolecular polymerization [30–52]. In search of a simpler model that can be used in more than one laboratory for helical self-organization and supramolecular polymerization experiments, we report here one of the simplest and most accessible self-assembling dendron. Additional examples of self-assembling dendrons and dendrimers already employed in related but incomplete studies, mostly from our laboratory, will also be discussed. Subsequently, some new, potentially interesting building blocks will be presented, and directions for the design of additional simple systems will be recommended.

Methods

Materials

1-Bromododecane (98%), thionyl chloride (99.5%), $LiAlH_4$ (95%), silica gel (60 Å, 32–63 μm) (Sorbent Technology), DMF, anhydrous K_2CO_3, (all from Fisher, ACS reagents) were used as received. Tetrahydrofuran (Fisher, ACS reagent grade) was refluxed over sodium/benzophenone and freshly distilled before use. Dichloromethane (Fisher, ACS reagent grade) was refluxed over CaH_2 and freshly distilled before use. All other chemicals were commercially available and were used as received.

Techniques

Nuclear magnetic resonance (NMR) spectroscopy

^{1}H NMR (500 MHz) and ^{13}C NMR (126 MHz) spectra were recorded on a Bruker DRX 500 instrument at 300K or other temperature indicated. Chemical shifts (δ) are reported in ppm and coupling constants (J) are reported in Hertz (Hz). The resonance multiplicities in the ^{1}H NMR spectra are described as "s" (singlet), "d" (doublet), "t" (triplet), "quint" (quintet) and "m" (multiplet) and broad resonances are indicated by "br". Residual protic solvent of $CDCl_3$ (^{1} H, δ 7.26 ppm; ^{13}C, δ 77.23 ppm, middle of the triplet), and tetramethylsilane (TMS, δ 0 ppm) were also used as the internal reference in the ^{1}H and ^{13}C spectra.

Thin-layer chromatography (TLC) and high-pressure liquid chromatography (HPLC)

The purity of the products was determined by a combination of thin-layer chromatography (TLC) on silica gel coated aluminum plates (with F_{254} indicator; layer thickness, 200 μm; particle size, 2–25 μm; pore size 60 Å, SIGMA-Aldrich) and high pressure liquid chromatography (HPLC) using THF as mobile phase at 1 mL/min, on a Shimadzu LC-10AT high pressure liquid chromatograph equipped with a Perkin Elmer LC-100 oven (40 °C), containing two Perkin-Elmer PL gel columns of 5×10^2 and 1×10^4 Å, a Shimadzu SPD-10A UV detector (λ = 254 nm), a Shimadzu RID-10A RI-detector, and a PE Nelson Analytical 900 Series integrator data station.

Differential scanning calorimetry (DSC)

Thermal transitions was carried out on a TA Instruments Q100 differential scanning calorimeter (DSC) equipped with a refrigerated cooling system with 10 °C min^{-1} heating and cooling rates. Indium was used as calibration standard. The transition temperatures were calculated as the maxima and minima of their endothermic and exothermic peaks. An Olympus BX51 optical microscope (100 X magnifications) equipped with a Mettler FP82HT hot stage and a Mettler Toledo FP90 Central Processor was used to verify thermal transitions and to characterize anisotropic textures. Melting points were measured using a uni-melt capillary melting point apparatus (Arthur H. Thomas Company) and were uncorrected. Density (ρ_{20}) measurements were carried out by flotation in gradient columns at 20 °C.

Matrix-assisted laser desorption/ionization time-of-flight (MALDI-TOF)

Matrix-assisted laser desorption/ionization time-of-flight (MALDI-TOF) mass spectrometry was performed on a PerSeptive Biosystems-Voyager-DE (Framingham, MA) mass spectrometer equipped with a nitrogen laser (337 μm) and operating in linear mode. Internal calibration was performed using Angiotensin II and Bombesin as standards. The analytical sample was obtained by mixing the THF solution of the sample (5–10 mg/ml) and THF solution of the matrix (3,5-dimethoxy-4-hydroxy-*trans*-cinnamic acid or 4-hydroxybenzylidenemalononitrile, 10 mg/mL) in a 1/5 v/v ratio. The prepared solution of the sample and the matrix (0.5 μL) was loaded on the MALDI plate and allowed to dry at 23 °C before the plate was inserted into the vacuum chamber of the MALDI instrument. The laser steps and voltages applied were adjusted depending on both the molecular weight and the nature of each analyzed compound.

Circular dichroism (CD) and UV measurements

Circular dichroism (CD) and UV spectroscopy measurements were carried out in a Jasco J-720 Spectropolarimeter integrated with Thermo Neslab RTE-111 refrigerated circulator digital temperature controller. Methyl cyclohexane, dodecane and butanol (spectrophotometric grade, 99%) were used as solvent.

X-ray diffraction (XRD)

X-ray diffraction (XRD) measurements were performed using Cu-$K_{\alpha 1}$ radiation (λ = 1.54178 Å) from a Bruker-Nonius FR-591

rotating anode X-ray source equipped with a 0.2 × 0.2 mm^2 filament operated at 3.4 kW. The Cu radiation beam was collimated and focused by a single bent mirror and sagitally focused through a Si (111) monochromator, generating in a 0.3 × 0.4 mm^2 spot on a Bruker-AXS Hi-Star multiwire area detector. To minimize attenuation and background scattering, an integral vacuum was maintained along the length of the flight tube and within the sample chamber. Samples were held in quartz capillaries (0.7–1.0 mm in diameter), mounted in a temperature-controlled oven (temperature precision: ± 0.1 °C, temperature range from -120 to 270 °C). The distance between the sample and the detector was 12.0 cm for wide angles diffraction experiments and 54.0 cm for intermediate angles diffraction experiments respectively. Aligned samples for fiber XRD experiments were prepared using a custom-made extrusion device. The powdered sample (∼ 10 mg) was heated inside the extrusion device above isotropization temperature. After slow cooling from the isotropic phase, the fiber was extruded in the liquid crystal phase and cooled to 23 °C. Typically, the aligned samples have a thickness of ∼ 0.3–0.7 mm and a length of ∼ 3–7 mm. All XRD measurements were done with the aligned sample axis perpendicular to the beam direction. XRD peaks position and intensity analysis was performed using Datasqueeze Software (version 2.01) [53] that allows background elimination and Gaussian, Lorentzian, Lorentzian squared, or Voigt peak-shape fitting. Molecular modeling calculations were done using the Materials Studio Modeling version 3.1 software from Accelrys. The package Discover module was used to perform the energy minimizations on the supramolecular structures with the following settings: PCFF or COMPASS force fields and Fletcher-Reeves algorithm for the conjugate gradient method.

Synthesis

Compounds **1** [54,55], **3a, 4a, 5a** [55] **3b, 4b, 5b,** and **7a**, the last with the short name **(4Bp-3,4)12G1CO$_2$CH$_3$** [45] were previously reported but were not completely structurally characterized by X-ray analysis. They were synthesized by employing procedures elaborated by Percec laboratory that were mentioned above. (*S*)-1-Bromo-3,7-dimethyloctane was synthesized by a procedure reported by Trzaska et al. [56].

3,4-Bis-[4′-((*S*)-3,7-dimethyl-octyloxy)-biphenyl-4-ylmethoxy]-benzoic acid methyl ester, (4Bp-3,4)dm8*G1CO$_2$CH$_3$, 7b: Methyl 3,4-dihydroxybenzoate, **6,** (0.64 g, 3.8 mmol) was added to a thoroughly degassed suspension of K_2CO_3 (2.1 g, 15.2 mmol) in DMF (50 mL) and the mixture was heated to 80 °C after which (4Bp)dm8*G0-CH_2Cl, **5b**, (2.73 g, 7.6 mmol) was added and the reaction was allowed to stir for 6 h at 80 °C under nitrogen. The reaction mixture was cooled to room temperature and poured into cold water (120 mL). The precipitate was collected by vacuum filtration and passed through a short column of basic alumina using CH_2Cl_2 as eluent. Recrystallization from acetone yielded 2.60 g (84%) of pure white solid of **(4Bp-3,4)dm8*G1CO$_2$CH$_3$, 7b**. HPLC: 99+%; TLC (EtOAc/hexane = 3/7): R_f = 0.24; MALDI-TOF analysis of both **(4Bp-3,4)12G1CO$_2$CH$_3$, 7a**, reported in Ref. [45], and **(4Bp-3,4)dm8*G1CO$_2$CH$_3$, 7b**, showed molar mass values equal to their theoretical, thus supporting their correct structures as indicated also by their NMR analysis. ^{1}H NMR (500 MHz, $CDCl_3$, 27°C, TMS): δ = 0.92 (d, 12H, J = 6.6 Hz), 1.00 (d, 6H, J = 6.6 Hz), 1.18–1.23 (m, 6H), 1.33-1.40 (m, 6H), 1.53–1.57 (m, 2H), 1.59–1.67 (m, 2H), 1.69–1.74 (m, 2H), 1.84–1.90 (m, 2H), 3.91 (s, 3H), 4.04–4.09 (m, 4H), 5.29 (s, 4H), 6.98–7.02 (overlapped peaks, 5H), 7.50–7.60 (overlapped peaks, 12H), 7.67–7.70 (dd, 1H, J = 6.4, 2.0 Hz), 7.73 (d, 1H, J = 2.0 Hz); ^{13}C NMR (125 MHz, 27°C, $CDCl_3$): δ = 19.9, 22.8, 22.9, 24.9, 28.2, 29.9, 30.1, 36.5, 37.5, 39.5, 52.2, 66.6, 70.9, 71.3, 113.6, 115.0, 115.8, 123.3, 124.3, 127.0, 127.1, 127.9, 128.2, 128.3, 128.6, 133.2, 133.3, 135.0, 135.3, 140.8, 148.6, 153.2, 159.0, 167.0. MALDI-TOF m/z: 812.6 ($[M]^+$, calculated for $C_{54}H_{68}O_6$ 812.5), 835.7 ($[M+Na]^+$, calculated 835.5).

Results and discussion

Fig. 1 outlines the synthesis of the first generation self-assembling dendron **(4Bp-3,4)nG1CO$_2$CH$_3$, 7a**. Compound **1** was alkylated with either 1-bromododecane or with the chiral (S)1-bromo-2,7-dimethyloctane (dm8*Br) in DMF at 80 °C in the presence of K_2CO_3 as base for 6 h to produce **3a** and **3b** in 93 and 95% isolated yield. Reduction of **3a** and **3b** with $LiAlH_4$ in THF at 0–23 °C for 2 h generated **4a** and **4b** in 88 and 94% isolated yield. Chlorination of the **4a** and **4b** with $SOCl_2$ in CH_2Cl_2 with a catalytic amount of DMF gave **5a** and **5b** in 89 and 94% isolated yield after 0.5 h at 0 to 23 °C. Alkylation of **6** with **5a** and **5b** in DMF at 80 °C in DMF with K_2CO_3 as base yielded **(4Bp-3,4)12G1CO$_2$CH$_3$, 7a**, and **(4Bp-3,4)dm8*G1CO$_2$CH$_3$, 7b**, in 90% and 84% isolated yields after 0.5h reaction time. This simple sequence of four, almost quantitative reaction steps, produced the achiral **(4Bp-3,4)12G1CO$_2$CH$_3$, 7a**, and the chiral **(4Bp-3,4)dm8*G1CO$_2$CH$_3$, 7b**, self-assembling dendrons. When the compound **1** from Fig. 1 was replaced with the corresponding methyl 4-hydroxybenzoate the resulting dendron formed only a crystal phase that was not determined by X-ray analysis [40]. This demonstrates the key role of replacing methyl 4-hydroxybenzoate with **1** during the synthesis described in Fig. 1.

The differential scanning calorimetry (DSC) analysis of the supramolecular structures resulted from **(4Bp-3,4)12G1CO$_2$CH$_3$, 7a**, and **(4Bp-3,4)dm8*G1CO$_2$CH$_3$, 7b**, complemented by fiber X-ray diffraction structural analysis experiments demonstrated their self-organization into helical columns forming crystal states in both cases (Fig. 2). The helical structure of the columns was supported by X-ray analysis, ~~to~~ that will be discussed later. DSC traces (Fig. 2, Tables 1 and 2) indicate that **(4Bp-3,4)12G1CO$_2$CH$_3$, 7a,** exhibits three distinguished phases before undergoing isotropization at 166.5 °C. During the first heating scan, below 73°C, **(4Bp-3,4)12G1CO$_2$CH$_3$, 7a**, as obtained from solution by precipitation, self-organizes first in a smectic phase (**S**). From 73 to 141.4 °C a helical crystalline columnar hexagonal phase (Φ_h^k) was found, and from 141.4 to 165.5 °C, a 2D center columnar rectangular phase (Φ_{r-c}) was observed. The Φ_{r-c} phase was stable until the isotropization temperature. However, during the first cooling and subsequent heating and cooling scans, the smectic phase does not appear again. During the first cooling below 128.2 ° and during the second heating below 141.2 °C, the crystalline columnar hexagonal phase (Φ_h^k) and the center columnar rectangular

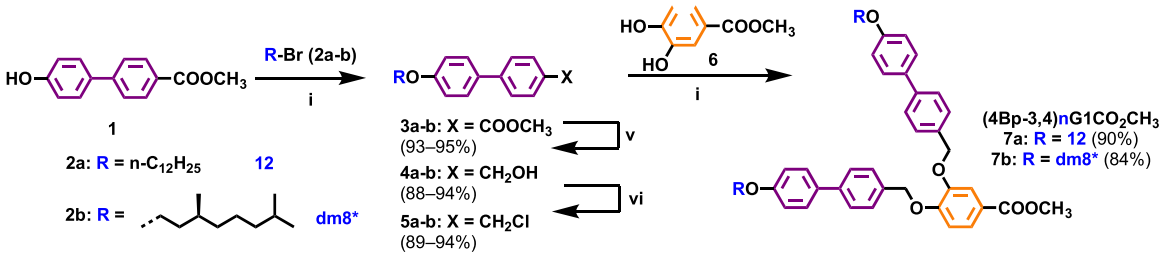

Fig. 1

Synthesis of hybrid dendrons **(4Bp-3,4)nG1CO$_2$CH$_3$, 7**, with achiral linear, **7a**, and chiral branched, **7b**, alkyl chains. Reagents and conditions: (i) K_2CO_3, DMF, 80 °C, 6 h; (ii) $LiAlH_4$, THF, 0–23 °C, 2 h; (iii) $SOCl_2$, DMF (cat.), DCM, 0–23 °C, 0.5 h.

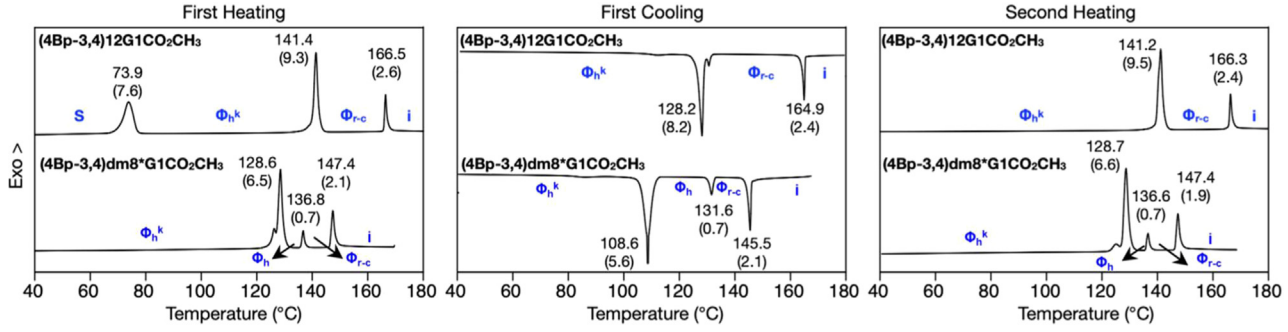

Fig. 2

DSC trances of **(4Bp-3,4)12G1CO$_2$CH$_3$, 7a**, achiral dendron and **(4Bp-3,4)dm8*G1CO$_2$CH$_3$, 7b,** chiral dendron. Scanning rate was 10 °C/min. S: smectic phase. $\Phi_h{}^k$: crystalline ordered hexagonal columnar lattice (p6mm space group), $\Phi_{r\text{-}c}$: centered rectangular columnar lattice, i: isotropic. Transition temperatures are in °C while enthalpy changes, in between parenthesis, are in Kcal/mole.

Table 1

Lattice Parameters and d-Spacings Obtained by the X-ray Analysis of the Supramolecular Assemblies of (4Bp-3,4)nG1CO$_2$CH$_3$, 7.

n [a]	T [°]	phase	lattice parameters a, b [b]; a [c] [Å]	$d_{11}, d_{20}, d_{02}, d_{31}, d_{22}, d_{40}$ [g] $d_{10}, d_{11}, d_{20}, d_{21}, d_{30}$ [h] $d_{10}, d_{20}, d_{30}, d_{40}$ [i]
12	25 [d]	S	60.2 [c]	60.2, 30.4, 20.1 [i]
	32	$\Phi_h{}^k$	68.9 [c]	59.9, 34.3, 29.9, 22.6, 19.9 [h]
	120	Φ_h	75.5 [c]	61.1, 35.3, 30.6, –, – [h]
	150	$\Phi_{r\text{-}c}$	63.1, 45.3 [b]	36.9, 31.3, 22.6, –, 18.5 [g]
dm8*	33	$\Phi_h{}^k$	65.2 [c]	56.7, 32.4, 28.2, 21.3, 18.8 [h]
	135	Φ_h	66.9 [c]	58.0, 33.5, 29.0, –, – [h]
	145	$\Phi_{r\text{-}c}$	105.9, 68.2 [b]	56.2, 56.2, 34.1, 31.4, 28.7, 26.5 [g]

[a] number of methylenic units in the alkyl chain;
[b] centered rectangular lattice ***a*** and ***b*** parameters;
[c] lattice parameter ***a***;
[d] phase observed only in the as prepared sample first heating;
[g] d-spacing for the centered rectangular phase. S: smectic phase. $\Phi_h{}^k$: crystalline ordered hexagonal columnar lattice (p6mm space group), $\Phi_{r\text{-}c}$: centered rectangular columnar lattice.[e] d-spacing of the lamellar phase;[f] d-spacing for the columnar hexagonal phase;

phase $\mathbf{\Phi_{r-c}}$ were formed. Preliminary X-Ray analysis data reported previously [45] for **(4Bp-3,4)12G1CO$_2$CH$_3$, 7a**, incorrectly assigned this $\mathbf{\Phi_h{}^k}$ phase to a columnar hexagonal phase with intracolumnar order ($\mathbf{\Phi_h{}^{io}}$). Also the high temperature $\mathbf{\Phi_{r-c}}$ phase was not previously assigned and therefore, it was marked as an unknown columnar **X**, $\mathbf{\Phi_x}$, phase [45].

DSC traces (Fig. 2, Tables 1 and 2) indicate that **(4Bp-3,4)dm8*G1CO$_2$CH$_3$, 7b**, exhibits three different phases before isotropization at 147.4 °C. During the first heating, below 128.6 °C, we observe a helical $\mathbf{\Phi_h{}^k}$ and from 128.6 to 136.8 °C, a 2D liquid crystalline hexagonal columnar phase ($\mathbf{\Phi_h}$) is formed just before the transition to the center columnar rectangular phase ($\mathbf{\Phi_{r-c}}$) that is stable up to the isotropization transition at 147 °C. It is remarkable to observe that the range of temperatures of all these helical self-organizations is in the range accessible by conventional X-ray diffraction techniques.

It is also extremely important and unexpected that the incorporation of the two methyl substituents in the chiral alkyl

Table 2

Structural and Retrostructural Analysis of the Columnar Hexagonal Phase Self-Organized from (4Bp-3,4)nG1CO$_2$CH$_3$, 7.

n [a]	T [°]	$a = D_{col}$ [b] [Å]	d_{10} [c] (A_{10} [d]), d_{11} (A_{11}), d_{20} (A_{20}), d_{21} (A_{21}), d_{30} (A_{30})	ρ [e] [g/cm^3]	μ [f]	D_{pore} [Å]
12	29	68.9	59.9 (33.76), 34.3 (32.98), 29.9 (26.64), 22.6 (3.30), 19.9 (3.31)	1.08	14.0	17.6 ± 4.0
dm8*	29	65.2	56.7 (33.87), 32.4 (33.16), 28.2 (26.83), 21.3 (2.12), 18.8 (4.03)	1.086	13.5	16.6 ± 2.0

[a] number of methylenic units in the alkyl chain;
[b] columnar hexagonal phase lattice parameter, error ±0.4 Å;
[c] X-ray diffraction measured d-spacing;
[d] diffraction peak scaled amplitude;
[e] experimental density measured at 20 °C, error is ±1%;
[f] number of dendrons per column stratum calculated from $\mu = VN_A t \rho / M_{wt}$, where V=unit cell volume=$a^3\sqrt{3}/2$, N_A=Avogadro number, t = 4.5 Å column stratum average thickness, M_{wt}=molecular weight, estimated error $\Delta\mu = \pm 10\%$.

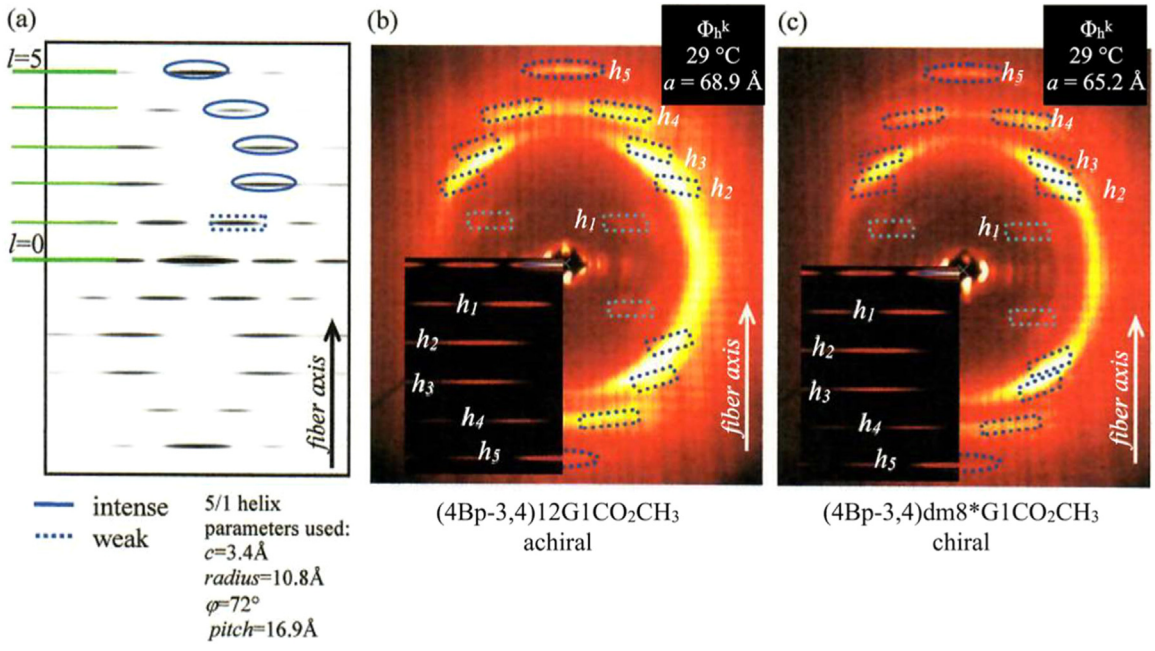

Fig. 3

Simulated 5/1 helix fiber pattern (a) and the experimental X-ray diffraction fiber pattern collected for the **(4Bp-3,4)12G1CO$_2$CH$_3$, 7a**, achiral dendron (b) and **(4Bp-3,4)dm8*G1CO$_2$CH$_3$, 7b**, chiral dendron (b). No signal changes were observed between the fiber data of the chiral and achiral molecules.

group of **(4Bp-3,4)dm8*G1CO$_2$CH$_3$, 7b**, lower phase transition temperatures but maintains the same sequence of helical self-organizations as in the case of **(4Bp-3,4)12G1CO$_2$CH$_3$, 7a**, except for the new Φ_h phase that appears in a very narrow range of temperatures between the Φ_h^k and the Φ_{r-c} phases (Fig. 2). Maintaining the helical supramolecular structure upon the incorporation of stereocenters in the original achiral building block is one of the most important and remarkable features of this self-assembling dendron.

The d-spacings and lattice parameters collected from X-ray diffraction experiments are summarized in Table 1. Table 2 summarizes also the experimental densities and the dimensions of the porous helical columns presented in Table 1. The number of the dendrons forming the cross-section of the helical column, μ, is also reported in Table 2. Characteristic X-ray diffraction pattern data at 29 °C during the first cooling and second heating scans of **(4Bp-3,4)12G1CO$_2$CH$_3$,7a**, have been summarized in Table 2. XRD patterns at 29 °C (Fig. 3, Table 2) indicate a columnar hexagonal crystalline phase (Φ_h^k). The presence of off axis diffraction patterns (Fig. 3) demonstrate that this is a crystalline columnar hexagonal phase. Its lattice parameters obtained at 29 °C are $a = b = 68.9$ Å. The measured d-spacings are shown on Table 2. From the known molecular weight (M_{wt}) 869.2 g.mol^{-1}, we calculate that the average number of dendrons forming the supramolecular column stratum with thickness (t), $\mu = N_A A t \rho / M_{wt}$ where $N_A = 6.022 \times 10^{23}$ mol^{-1} = Avogadro's number, A is the area of the column cross-section calculated from the lattice parameters ($A = \sqrt{3}/2 \times a^2$), ρ is the density of the compound, t is the stratum thickness. From this calculation, we find that for the Φ_h^k phase, there must be fifteen dendron molecules ($\mu = 14 \sim 15$) per stratum. The column diameter is 68.9 Å ($D_{col} = a$). The c-axis of the phase is along the fiber axis. The XRD pattern (Fig. 3) indicates that we are dealing with a 5/1 helix. Calculations demonstrate that there must be three dendron molecules per cross-section supramolecular column layer.

The X-ray diffraction patterns obtained at 29 °C for **(4Bp-3,4)dm8*G1CO$_2$CH$_3$,7b**, have been summarized in Table 2. XRD patterns 29 °C (Fig. 3, Table 2) indicate a helical Φ_h^k phase, that is supported by the presence of off-axis diffraction pattern (Fig. 3). The lattice parameters at 29 °C are $a = b = 65.2$ Å. The measured *d*-spacings are shown in Table 2. From the value of the molecular weight (M_{wt}) 799.1 g.mol^{-1}, we determine an average number of self-assembling dendrons forming the supramolecular column stratum with thickness (t), μ This calculation was done with the methodology reported above in more details for the supramolecular structure assembled from the achiral dendron **(4Bp-3,4)12G1CO$_2$CH$_3$,7a**, and demonstrated that ~~for~~ the Φ_h^k phase, contains fifteen self-assembling dendron molecules ($\mu = 13.5 \sim 15$) per stratum. The column diameter is 65.2 Å [$D_{col} = a$]. The *c*-axis of the phase is along the fiber axis. ~~As~~ The XRD pattern (Fig. 3) again demonstrates that it is a 5/1 helix with three dendrons per layer.

Fig. 3a presents the simulated X-ray fiber patterns of the helical self-organizations of achiral **(4Bp-3,4)12G1CO$_2$CH$_3$, 7a**, and chiral **(4Bp-3,4)dm8*G1CO$_2$CH$_3$, 7b**. A 5/1 helical column was formed both by the achiral and the chiral dendrons. This remarkable result demonstrates that the stereocenter from the alkyl groups of **(4Bp-3,4)dm8*G1CO$_2$CH$_3$, 7b**, does not induce helicity in the achiral column of **(4Bp-3,4)12G1CO$_2$CH$_3$, 7a**, but that both the supramolecular columns of **(4Bp-3,4)12G1CO$_2$CH$_3$, 7a**, and of **(4Bp-3,4)dm8*G1CO$_2$CH$_3$, 7b**, are helical and that the stereocenter of **(4Bp-3,4)dm8*G1CO$_2$CH$_3$, 7b**, selects the helical sense of an already helical column. The model of the **(4Bp-3,4)12G1CO$_2$CH$_3$, 7a**, helical column is shown in Fig. 4.

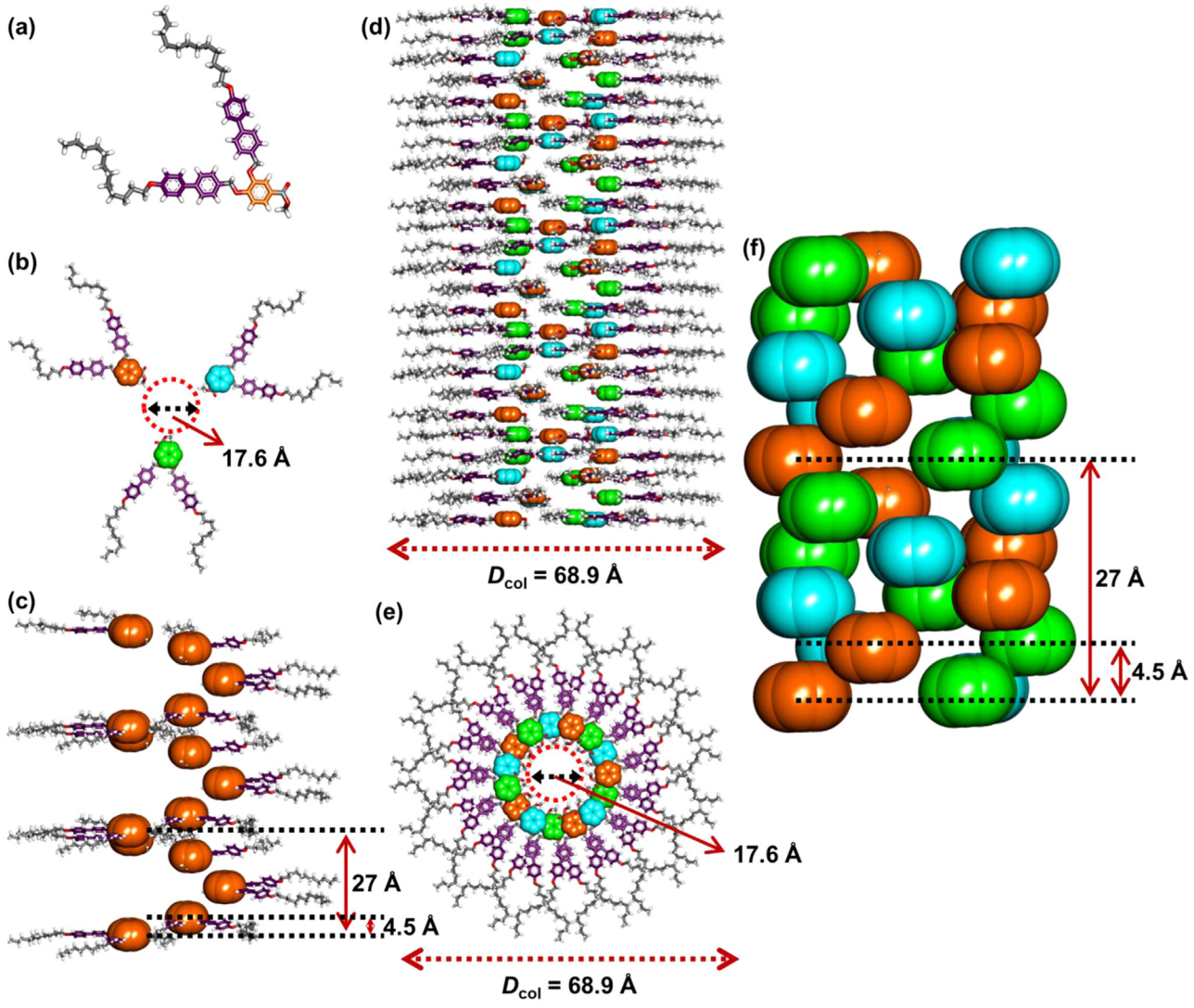

Fig. 4

Molecular models of **(4Bp-3,4)12G1CO$_2$CH$_3$, 7a**, at 32 °C (Φ_h^k phase). (a) Single dendron (Top View); (b) One layer of the column (Φ_h^k phase) formed by three molecules (Top View); (c) One strand of the column showing the helicity (5/1 helix); (d) Formation of the column by stacking of the layers with a distance of 4.5 Å and 72° rotation along the fiber axis (Side View); (e) Single column (Top View); (f) Core view (Side View) showing the helicity (5/1). Color code used in the model: O atoms, red; H atoms, white; C atoms in the phenyl rings, brown, green, and blue; C atoms in the biphenyl rings, yellow; all other C atoms, grey. In (f) Biphenyl groups, alkyl groups (–$C_{12}H_{25}$), and H atoms are deleted for clarity.

Fig. 4a–f shows the molecular models for the Φ_h^k phase. For Φ_h^k phase the repeat unit is formed by three molecules (Fig. 4b). In the first step, three molecules are placed with an angle of 120° symmetrically with distorted alkyl chains ($-C_{12}H_{25}$) (Fig. 4b) to form a layer. In the second step, another layer is placed on top of the first layer at 4.5 Å but is rotated by 72° (Fig. 4c, d). Thus, each layer will stack over one another with a rotation of 72° to form the column (Fig. 4d, e) with three strands 5/1 helicity. To show the formation of one helix in the three strand helices, one strand is shown in Fig. 4c for clarity. The core of three helices of the 5/1 helix column is shown in Fig. 4f. Then these columns will arrange themselves in the helical crystalline hexagonal array (Φ_h^k). A slightly different model that fits in an identical way the X-ray diffraction experiments is shown in Fig. S1 (Supplemental Information). Fig. 5 shows the helical self-organization monitored by a combination of CD and UV in 1-butanol. No self-assembly was observed in methyl cyclohexane and in dodecane. Again, in solution as in bulk state, preliminary experiments demonstrated that the self-organization occurs in a very reasonable range of temperatures in 1-butanol. Due to some unexpected CD instrument problems that could not be yet resolved, no experiments are available at this time to compare the helical structure in bulk state with the one obtained in solution. When these experiments will become available, they will be reported to confirm the persistence of the helical structure between bulk and solution states as demonstrated previously in different helical systems reported from our laboratory [1,6,12–29].

Self-assembling dendrons **(4Bp-3,4)12G1CO$_2$CH$_3$, 7a**, and **(4Bp-3,4)dm8*G1CO$_2$CH$_3$, 7b**, provide a large diversity of opportunities in the field of helical self-organization and supramolecular polymerization. Their alkyl groups can be achiral, racemic, or chiral and their number of carbons can be altered without requesting unusual organic synthesis expertise. Stereocenters can be incorporated on the periphery of **(4Bp-3,4)nG1CO$_2$CH$_3$, 7**, as is in the case of **(4Bp-3,4)dm8*G1CO$_2$CH$_3$, 7b**, but at the same time the stereocenter can be incorporated at the apex only, at the apex and on the periphery. This manipulation of the position and nature of the stereocenter provides numerous opportunities to investigate and elucidate fundamental aspect of helical self-organization. The biphenyl part of the dendron can also be changed into a naphthyl derivative and the same sequence of self-organization processes is expected to occur. We also can think about changing the biphenyl part of **(4Bp-3,4)nG1CO$_2$CH$_3$, 7**, into a dibenzyl ether as shown already in other publications from our laboratory [42,47]. Aside from the simple chemical modifications mentioned above we expect that chemical functionalization of this self-assembling dendron at its apex with dipeptides [1], crown ethers [57–60], podants [61,62] and electronically active components [63,64] will provide access to Aquaporin-like channels for water separation and purification [1,6,65], ionically active components [58] and self-repairing organic electronics [63] that previously did not provide the same high level of helical order as the very simple supramolecular dendrimer system reported here. The fact that self-assembling dendrons are true monomers while discotic self-assembling components are oligomeric species such as dimers, trimers, tetramers and even higher oligomers [66–84] is expected to provide access to a more detailed analysis of the helical self-organization and supramolecular polymerization process. Last but not least, this self-assembling dendron compliments previous experiments reported on the elucidation of the role of molecular parameters of the building block on helical self-organization [52,66-87]. We expect that the simplicity and the rich diversity of potential structural variations transform this very

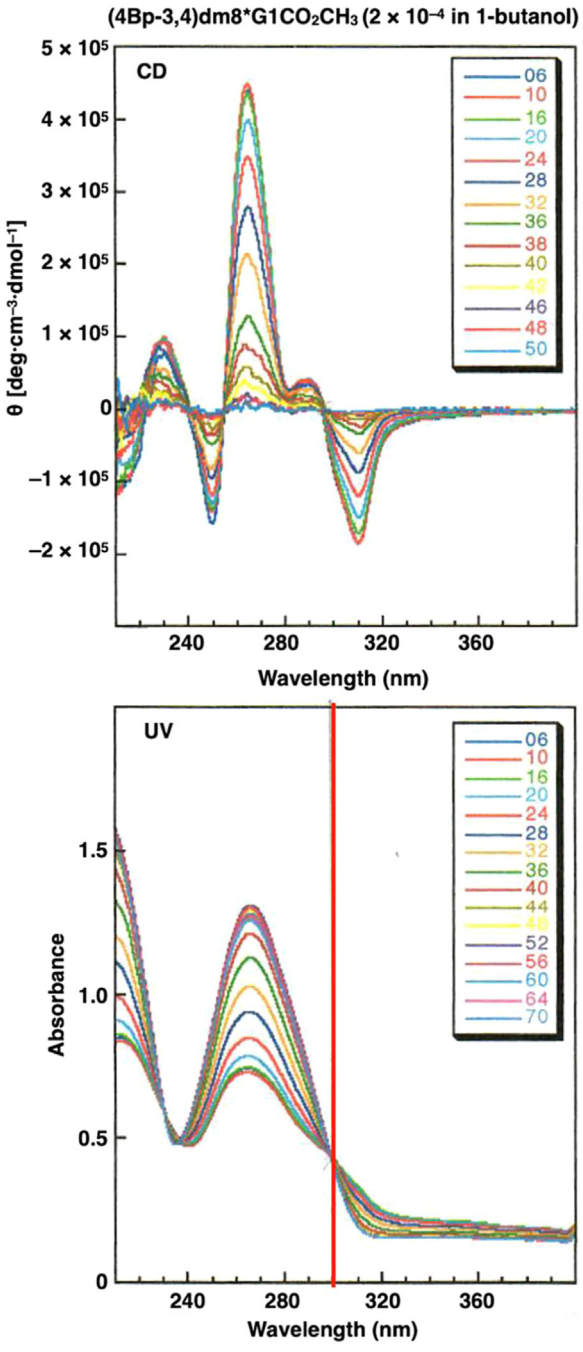

Fig. 5

CD (top) and UV (bottom) spectra of **(4Bp-3,4)dm8*G1CO$_2$CH$_3$, 7b**, during its temperature-dependent self-assembly in 1-butanol at different temperatures indicated in °C. CD signal means helical supramolecular column, while flat CD represents molecular solution of the dendron.

simple first generation self-assembling dendron into an important contributor to the field of helical self-organization.

Conclusions

An extremely simple first generation self-assembling dendron undergoing helical self-organization in solution and bulk state regardless of the presence or absence of a stereocenter in its structure was reported. This first generation dendron can undergo a large diversity of structural modifications, all maintaining its helical self-organization in bulk state and in solution in a range of temperature of great interest for the current instrumentation employed to study supramolecular polymerization in bulk state and in solution. We expect that this self-assembling dendron has the potential to become an important contributor to the field of helical self-organization.

Declaration of Competing Interest

The authors declare that they have no known competing financial interests or personal relationships that could have appeared to influence the work reported in this paper.

Data Availability

No data was used for the research described in the article.

Acknowledgments

Financial support by the National Science Foundation (DMR-1807127, DMR-1720530, and DMR- 2104554), the Humboldt Foundation, and the P. Roy Vagelos Chair at Penn (all to V.P.) is gratefully acknowledged.

Supplementary materials

Supplementary material associated with this article can be found, in the online version, at doi:10.1016/j.giant.2022.100118.

References

[1] V. Percec, A.E. Dulcey, V.S.K. Balagurusamy, Y. Miura, J. Smidrkal, M. Peterca, S. Nummelin, U. Edlund, S.D. Hudson, P.A. Heiney, H. Duan, S.N. Magonov, S.A. Vinogradov, Self-assembly of amphiphilic dendritic dipeptides into helical pores, Nature 430 (2004) 764–768, doi:10.1038/nature02770.

[2] V. Percec, A.E. Dulcey, M. Peterca, M. Ilies, J. Ladislaw, B.M. Rosen, U. Edlund, P.A. Heiney, The internal structure of helical pores self-assembled from dendritic dipeptides is stereochemically programmed and allosterically regulated, Angew. Chem. Int. Ed. 44 (2005) 6516–6521, doi:10.1002/anie.200501331.

[3] V. Percec, A.E. Dulcey, M. Peterca, M. Ilies, M.J. Sienkowska, P.A. Heiney, Programming the internal structure and stability of helical pores self-assembled from dendritic dipeptides via the protective groups of the peptide, J. Am. Chem. Soc. 127 (2005) 17902–17909, doi:10.1021/ja056313h.

[4] V. Percec, A. Dulcey, M. Peterca, M. Ilies, Y. Miura, U. Edlund, P.A. Heiney, V. Percec, A. Dulcey, M. Peterca, M. Ilies, Y. Miura, U. Edlund, P.A. Heiney, Helical porous protein mimics self-assembled from amphiphilic dendritic dipeptides, Aust. J. Chem. 58 (2005) 472–482, doi:10.1071/CH05092.

[5] M. Peterca, V. Percec, A.E. Dulcey, S. Nummelin, S. Korey, M. Ilies, P.A. Heiney, Self-assembly, structural, and retrostructural analysis of dendritic dipeptide pores undergoing reversible circular to elliptical shape change, J. Am. Chem. Soc. 128 (2006) 6713–6720, doi:10.1021/ja0611902.

[6] M.S. Kaucher, M. Peterca, A.E. Dulcey, A.J. Kim, S.A. Vinogradov, D.A. Hammer, P.A. Heiney, V. Percec, Selective transport of water mediated by porous dendritic dipeptides, J. Am. Chem. Soc. 129 (2007) 11698–11699, doi:10.1021/ja076066c.

[7] V. Percec, A.E. Dulcey, M. Peterca, M. Ilies, S. Nummelin, M.J. Sienkowska, P.A. Heiney, Principles of self-assembly of helical pores from dendritic dipeptides, Proc. Natl. Acad. Sci. USA. 103 (2006) 2518–2523, doi:10.1073/pnas.0509676103.

[8] V. Percec, A.E. Dulcey, M. Peterca, P. Adelman, R. Samant, V.S.K. Balagurusamy, P.A. Heiney, Helical pores self-assembled from homochiral dendritic dipeptides based on L-Tyr and nonpolar alpha-amino acids, J. Am. Chem. Soc. 129 (2007) 5992–6002, doi:10.1021/ja071088k.

[9] B.M. Rosen, M. Peterca, K. Morimitsu, A.E. Dulcey, P. Leowanawat, A.M. Resmerita, M.R. Imam, V. Percec, Programming the supramolecular helical polymerization of dendritic dipeptides via the stereochemical information of the dipeptide, J. Am. Chem. Soc. 133 (2011) 5135–5151, doi:10.1021/ja200280h.

[10] V. Percec, M. Peterca, A.E. Dulcey, M.R. Imam, S.D. Hudson, S. Nummelin, P. Adelman, P.A. Heiney, Hollow spherical supramolecular dendrimers, J. Am. Chem. Soc. 130 (2008) 13079–13094, doi:10.1021/ja8034703.

[11] V. Percec, P. Leowanawat, Why are biological systems homochiral? Isr. J. Chem. 51 (2011) 1107–1117, doi:10.1002/ijch.201100152.

[12] A.J. Kim, M.S. Kaucher, K.P. Davis, M. Peterca, M.R. Imam, N.A. Christian, D.H. Levine, F.S. Bates, V. Percec, D.A. Hammer, Proton transport from dendritic helical-pore-incorporated polymersomes, Adv. Funct. Mater. 19 (2009) 2930–2936, doi:10.1002/adfm.200900076.

[13] V. Percec, Bioinspired supramolecular liquid crystals, Philos. Trans. R. Soc. A 364 (2006) 2709–2719, doi:10.1098/rsta.2006.1848.

[14] W. Song, C. Lang, Y. Shen, M. Kumar, Design considerations for artificial water channel–based membranes, Annu. Rev. Mater. Res. 48 (2018) 57–82, doi:10.1146/annurev-matsci-070317-124544.

[15] Y.J. Lim, K. Goh, R. Wang, The coming of age of water channels for separation membranes: from biological to biomimetic to synthetic, Chem. Soc. Rev. 51 (2022) 4537–4582, doi:10.1039/D1CS01061A.

[16] L.B. Huang, M. Di Vincenzo, Y. Li, M. Barboiu, Artificial water channels: towards biomimetic membranes for desalination, Chem. Eur. J. 27 (2021) 2224–2239, doi:10.1002/chem.202003470.

[17] L.B. Huang, M. Di Vincenzo, M.G. Ahunbay, A. van der Lee, D. Cot, S. Cerneaux, G. Maurin, M. Barboiu, Bilayer versus polymeric artificial water channel membranes: structural determinants for enhanced filtration performances, J. Am. Chem. Soc. 143 (2021) 14386–14393, doi:10.1021/jacs.1c07425.

[18] M. Di Vincenzo, A. Tiraferri, V.E. Musteata, S. Chisca, R. Sougrat, L.B. Huang, S.P. Nunes, M. Barboiu, Biomimetic artificial water channel membranes for enhanced desalination, Nat. Nanotechnol. 16 (2021) 190–196, doi:10.1038/s41565-020-00796-x.

[19] T. Jiang, A. Hall, M. Eres, Z. Hemmatian, B. Qiao, Y. Zhou, Z. Ruan, A.D. Couse, W.T. Heller, H. Huang, M.O. de la Cruz, M. Rolandi, T. Xu, Single-chain heteropolymers transport protons selectively and rapidly, Nature 577 (2020) 216–220, doi:10.1038/s41586-019-1881-0.

[20] Y. Chen, H.Y. Chang, M.T. Lee, Z.R. Yang, C.H. Wang, K.Y. Wu, W.T. Chuang, C.L. Wang, Dual-axis alignment of bulk artificial water channels by directional water-induced self-assembly, J. Am. Chem. Soc. 144 (2022) 7768–7777, doi:10.1021/jacs.2c00929.

[21] J. Shen, A. Roy, H. Joshi, L. Samineni, R. Ye, Y.M. Tu, W. Song, M. Skiles, M. Kumar, A. Aksimentiev, H. Zeng, Fluorofoldamer-based salt- and proton-rejecting artificial water channels for ultrafast water transport, Nano Lett. 22 (2022) 4831–4838, doi:10.1021/acs.nanolett.2c01137.

[22] A. Roy, J. Shen, H. Joshi, W. Song, Y.M. Tu, R. Chowdhury, R. Ye, N. Li, C. Ren, M. Kumar, A. Aksimentiev, H. Zeng, Foldamer-based ultrapermeable and highly selective artificial water channels that exclude protons, Nat. Nanotechnol. 16 (2021) 911–917, doi:10.1038/s41565-021-00915-2.

[23] Y. Shen, W. Si, M. Erbakan, K. Decker, R. De Zorzi, P.O. Saboe, Y.J. Kang, S. Majd, P.J. Butler, T. Walz, A. Aksimentiev, J. Hou, M. Kumar, Highly permeable artificial water channels that can self-assemble into two-dimensional arrays, Proc. Natl. Acad. Sci. 112 (2015) 9810–9815, doi:10.1073/pnas.1508575112.

[24] Y. Itoh, S. Chen, R. Hirahara, T. Konda, T. Aoki, T. Ueda, I. Shimada, J.J. Cannon, C. Shao, J. Shiomi, K.V. Tabata, H. Noji, K. Sato, T. Aida, Ultrafast water permeation through nanochannels with a densely fluorous interior surface, Science 376 (2022) 738–743, doi:10.1126/science.abd0966.

[25] C. Roche, H.J. Sun, M.E. Prendergast, P. Leowanawat, B.E. Partridge, P.A. Heiney, F. Araoka, R. Graf, H.W. Spiess, X. Zeng, G. Ungar, V. Percec, Homochiral columns constructed by chiral self-sorting during supramolecular helical organization of hat-ahaped molecules, J. Am. Chem. Soc. 136 (2014) 7169–7185, doi:10.1021/ja5035107.

[26] C. Roche, H.J. Sun, P. Leowanawat, F. Araoka, B.E. Partridge, M. Peterca, D.A. Wilson, M.E. Prendergast, P.A. Heiney, R. Graf, H.W. Spiess, X. Zeng, G. Ungar, V. Percec, A supramolecular helix that disregards chirality, Nat. Chem. 8 (2016) 80–89, doi:10.1038/nchem.2397.

[27] B.E. Partridge, L. Wang, D. Sahoo, J.T. Olsen, P. Leowanawat, C. Roche, H. Ferreira, K.J. Reilly, X. Zeng, G. Ungar, P.A. Heiney, R. Graf, H.W. Spiess, V. Percec, Sequence-defined dendrons dictate supramolecular cogwheel assembly of dendronized perylene bisimides, J. Am. Chem. Soc. 141 (2019) 15761–15766, doi:10.1021/jacs.9b08714.

[28] L. Wang, B.E. Partridge, N. Huang, J.T. Olsen, D. Sahoo, X. Zeng, G. Ungar, R. Graf, H.W. Spiess, V. Percec, Extraordinary acceleration of cogwheel helical self-organization of dendronized perylene bisimides by the dendron sequence encoding their tertiary structure, J. Am. Chem. Soc. 142 (2020) 9525–9536, doi:10.1021/jacs.0c03353.

[29] M.S. Ho, B.E. Partridge, H.J. Sun, D. Sahoo, P. Leowanawat, M. Peterca, R. Graf, H.W. Spiess, X. Zeng, G. Ungar, P.A. Heiney, C.S. Hsu, V. Percec, Screening libraries of semifluorinated arylene bisimides to discover and predict thermodynamically controlled helical crystallization, ACS Comb. Sci. 18 (2016) 723–739, doi:10.1021/acscombsci.6b00143.

[30] T. Aida, E.W. Meijer, S.I. Stupp, Functional supramolecular polymers, Science 335 (2012) 813–817, doi:10.1126/science.1205962.

[31] V. Percec, J. Heck, G. Johansson, D. Tomazos, M. Kawasumi, G. Ungar, Molecular-recognition-directed self-assembly of supramolecular polymers, J. Macromol. Sci. Part A Pure Appl. Chem. 31 (1994) 1031–1070, doi:10.1080/10601329409349776.

[32] V. Percec, G. Ungar, M. Peterca, Self-assembly in action, Science 313 (2006) 55–56, doi:10.1126/science.1129512.

[33] B.M. Rosen, C.J. Wilson, D.A. Wilson, M. Peterca, M.R. Imam, V. Percec, Dendron-mediated self-assembly, disassembly, and self-organization of complex systems, Chem. Rev. 109 (2009) 6275–6540, doi:10.1021/cr900157q.

[34] H.J. Sun, S. Zhang, V. Percec, From structure to function *via* complex supramolecular dendrimer systems, Chem. Soc. Rev. 44 (2015) 3900–3923, doi:10.1039/C4CS00249K.

[35] V. Percec, Q. Xiao, G. Lligadas, M.J. Monteiro, Perfecting self-organization of covalent and supramolecular mega macromolecules via sequence-defined and monodisperse components, Polymer 211 (2020) 123252, doi:10.1016/j.polymer.2020.123252.

[36] V. Percec, Merging macromolecular and supramolecular chemistry into bioinspired synthesis of complex systems, Isr. J. Chem. 60 (2020) 48–66, doi:10.1002/ijch.202000004.

[37] V. Percec, Q. Xiao, Helical self-organizations and emerging functions in architectures, biological and synthetic macromolecules, Bull. Chem. Soc. Jpn. 94 (2021) 900–928, doi:10.1246/bcsj.20210015.

[38] V. Percec, Q. Xiao, Helical chirality of supramolecular columns and spheres self-organizes complex liquid crystals, crystals, and quasicrystals, Isr. J. Chem. 61 (2021) 530–565, doi:10.1002/ijch.202100057.

[39] V. Percec, W.D. Cho, P.E. Mosier, G. Ungar, D.J.P. Yeardley, Structural analysis of cylindrical and spherical supramolecular dendrimers quantifies the concept of monodendron shape control by generation number, J. Am. Chem. Soc. 120 (1998) 11061–11070, doi:10.1021/ja9819007.

[40] V. Percec, W.D. Cho, G. Ungar, D.J.P. Yeardley, Synthesis and structural analysis of two constitutional isomeric libraries of AB_2-based monodendrons and supramolecular dendrimers, J. Am. Chem. Soc. 123 (2001) 1302–1315, doi:10.1021/ja0037771.

[41] V. Percec, M. Peterca, M.J. Sienkowska, M.A. Ilies, E. Aqad, J. Smidrkal, P.A. Heiney, Synthesis and retrostructural analysis of libraries of AB_3 and constitutional isomeric AB_2 phenylpropyl ether-based supramolecular dendrimers, J. Am. Chem. Soc. 128 (2006) 3324–3334, doi:10.1021/ja060062a.

[42] V. Percec, C.M. Mitchell, W.D. Cho, S. Uchida, M. Glodde, G. Ungar, X. Zeng, Y. Liu, V.S.K. Balagurusamy, P.A. Heiney, Designing libraries of first generation AB_3 and AB_2 self-assembling dendrons *via* the primary structure generated from combinations of $(AB)_y{-}AB_3$ and $(AB)_y{-}AB_2$ building blocks, J. Am. Chem. Soc. 126 (2004) 6078–6094, doi:10.1021/ja049846j.

[43] V. Percec, B.C. Won, M. Peterca, P.A. Heiney, Expanding the structural diversity of self-assembling dendrons and supramolecular dendrimers via complex building blocks, J. Am. Chem. Soc. 129 (2007) 11265–11278, doi:10.1021/ja073714j.

[44] V. Percec, M.R. Imam, M. Peterca, W.D. Cho, P.A. Heiney, Self-assembling dendronized dendrimers, Isr. J. Chem. 49 (2009) 55–70, doi:10.1560/IJC.49.1.55.

[45] M. Peterca, M.R. Imam, P. Leowanawat, B.M. Rosen, D.A. Wilson, C.J. Wilson, X. Zeng, G. Ungar, P.A. Heiney, V. Percec, Self-assembly of hybrid dendrons into doubly segregated supramolecular polyhedral columns and vesicles, J. Am. Chem. Soc. 132 (2010) 11288–11305, doi:10.1021/ja104432d.

[46] V. Percec, M.N. Holerca, S. Nummelin, J.J. Morrison, M. Glodde, J. Smidrkal, M. Peterca, B.M. Rosen, S. Uchida, V.S.K. Balagurusamy, M.J. Sienkowska, P.A. Heiney, Exploring and expanding the structural diversity of self-assembling dendrons through combinations of AB, constitutional isomeric AB_2, and AB_3 biphenyl-4-methyl ether building blocks, Chem. Eur. J. 12 (2006) 6216–6241, doi:10.1002/chem.200600178.

[47] V. Percec, J. Smidrkal, M. Peterca, C.M. Mitchell, S. Nummelin, A.E. Dulcey, M.J. Sienkowska, P.A. Heiney, Self-assembly of hybrid dendrons with complex primary structure into functional helical pores, Chem. A Eur. J. 13 (2007) 3989–4007, doi:10.1002/chem.200601582.

[48] B.M. Rosen, D.A. Wilson, C.J. Wilson, M. Peterca, B.C. Won, C. Huang, L.R. Lipski, X. Zeng, G. Ungar, P.A. Heiney, V. Percec, Predicting the structure of supramolecular dendrimers via the analysis of libraries of AB_3 and constitutional isomeric AB_2 biphenylpropyl ether self-assembling dendrons, J. Am. Chem. Soc. 131 (2009) 17500–17521, doi:10.1021/ja907882n.

[49] V. Percec, J.G. Rudick, M. Peterca, M.E. Yurchenko, J. Smidrkal, P.A. Heiney, Supramolecular structural diversity among first-generation hybrid dendrimers and twin dendrons, Chem. Eur. J. 14 (2008) 3355–3362, doi:10.1002/chem.200701658.

[50] B.M. Rosen, M. Peterca, C. Huang, X. Zeng, G. Ungar, V. Percec, Deconstruction as a strategy for the design of libraries of self-assembling dendrons, Angew. Chem. Int. Ed. 49 (2010) 7002–7005, doi:10.1002/anie.201002514.

[51] M. Peterca, M.R. Imam, C.H. Ahn, V.S.K. Balagurusamy, D.A. Wilson, B.M. Rosen, V. Percec, Transfer, Amplification, and inversion of helical chirality mediated by concerted interactions of C3-supramolecular dendrimers, J. Am. Chem. Soc. 133 (2011) 2311–2328 https://doiorg/10.1021/ja110753s.

[52] V. Percec, S. Wang, N. Huang, B.E. Partridge, X. Wang, D. Sahoo, D.J. Hoffman, J. Malineni, M. Peterca, R.L. Jezorek, N. Zhang, H. Daud, P.D. Sung, E.R. McClure, S.L. Song, An accelerated modular-orthogonal Ni-catalyzed methodology to symmetric and nonsymmetric constitutional isomeric AB2 to AB9 dendrons exhibiting unprecedented self-organizing principles, J. Am. Chem. Soc. 143 (2021) 17724–17743, doi:10.1021/jacs.1c08502.

[53] P.A. Heiney, Datasqueeze: a software tool for powder and small-angle X-ray diffraction analysis, Comm. Powder Diffr. Newsl. 32 (2005) 9–11.

[54] V. Percec, Q. Zheng, M. Lee, Molecular engineering of liquid-crystalline polymers by living polymerization. Part 13. – synthesis and living cationic polymerization of (S)-(–)-2-methylbutyl 4′-(ω-vinyloxy)alkoxybiphenyl-4-carboxylate with undecanyl and hexyl alkyl groups, J. Mater. Chem. 1 (1991) 611–619, doi:10.1039/JM9910100611.

[55] V. Percec, D. Schlueter, G. Ungar, S.Z.D. Cheng, A. Zhang, Hierarchical control of internal superstructure, diameter, and stability of supramolecular and macromolecular columns generated from tapered monodendritic building blocks, Macromolecules 31 (1998) 1745–1762, doi:10.1021/ma971459p.

[56] S.T. Trzaska, H.F. Hsu, T.M. Swager, Cooperative chirality in columnar liquid crystals: studies of fluxional octahedral metallomesogens, J. Am. Chem. Soc. 121 (1999) 4518–4519, doi:10.1021/ja9900609.

[57] V. Percec, G. Johansson, G. Ungar, J. Zhou, Fluorophobic effect induces the self-assembly of semifluorinated tapered monodendrons containing crown ethers into supramolecular columnar dendrimers which exhibit a homeotropic hexagonal columnar liquid crystalline phase, J. Am. Chem. Soc. 118 (1996) 9855–9866, doi:10.1021/ja9615738.

[58] V. Percec, G. Johansson, J. Heck, G. Ungarb, S.V. Battyb, Molecular recognition directed self-assembly of supramolecular cylindrical channel-like architectures from 6,7,9,10,12,13,15,16-octahydro-1,4,7,10,13-pentaoxa benzocyclopentadecen-2-ylmethyl 3,4,5-tris(p-dodecyloxybenzyloxy)benzoate, J. Chem. Soc. Perkin Trans. 1 (1993) 1411–1420, doi:10.1039/P19930001411.

[59] G. Johansson, V. Percec, G. Ungar, D. Abramic, Molecular recognition directed self-assembly of tubular liquid crystalline and crystalline supramolecular architectures from taper shaped (15-crown-5)methyl 3,4,5-tris(p-alkyloxybenzyloxy)benzoates and (15-crown-5)methyl 3,4,5-tris(p-dodecyloxy)benzoate, J. Chem. Soc. Perkin Trans. 1 (1994) 447–459, doi:10.1039/P19940000447.

[60] V. Percec, W.D. Cho, G. Ungar, D.J.P. Yeardley, Synthesis and NaOTf mediated self-assembly of monodendritic crown ethers, Chem. Eur. J. 8 (2002) 2011–2025, doi:10.1002/1521-3765(20020503)8:9<2011::AID-CHEM2011>3.0.CO;2-3.

[61] V. Percec, J.A. Heck, D. Tomazos, G. Ungar, The influence of the complexation of sodium and lithium triflate on the self-assembly of tubular-supramolecular architectures displaying a columnar mesophase based on taper-shaped monoesters of oligoethylene oxide with 3,4,5-tris[p-(n-dodecan-1-yloxy)benzyloxy]benzoic acid and of their polymethacrylates, J. Chem. Soc. Perkin Trans. 2 (1993) 2381–2388, doi:10.1039/P29930002381.

[62] V. Percec, D. Tomazos, J. Heck, H. Blackwell, G. Ungar, Self-assembly of taper-shaped monoesters of oligo(ethylene oxide) with 3,4,5-tris(n-dodecan-1-yloxy)benzoic acid and of their polymethacrylates into tubular supramolecular architectures displaying a columnar hexagonal mesophase, J. Chem. Soc. Perkin Trans. 2 (1994) 31–44, doi:10.1039/P29940000031.

[63] V. Percec, M. Glodde, T.K. Bera, Y. Miura, I. Shiyanovskaya, K.D. Singer, V.S.K. Balagurusamy, P.A. Heiney, I. Schnell, A. Rapp, H.W. Spiess, S.D. Hudson, H. Duan, Self-organization of supramolecular helical dendrimers into complex electronic materials, Nature 419 (2002) 384–387, doi:10.1038/nature01072.

[64] V. Percec, M. Glodde, M. Peterca, A. Rapp, I. Schnell, H.W. Spiess, T.K. Bera, Y. Miura, V.S.K. Balagurusamy, E. Aqad, P.A. Heiney, Self-assembly of semifluorinated dendrons attached to electron-donor groups mediates their π-stacking via a helical pyramidal column, Chem. Eur. J. 12 (2006) 6298–6314, doi:10.1002/chem.200501195.

[65] W. Song, M. Kumar, Artificial water channels: toward and beyond desalination, Curr. Opin. Chem. Eng. 25 (2019) 9–17, doi:10.1016/j.coche.2019.06.007.

[66] D. Miyajima, F. Araoka, H. Takezoe, J. Kim, K. Kato, M. Takata, T. Aida, Columnar liquid crystal with a spontaneous polarization along the columnar axis, J. Am. Chem. Soc. 132 (2010) 8530–8531, doi:10.1021/ja101866e.

[67] D. Miyajima, F. Araoka, H. Takezoe, J. Kim, K. Kato, M. Takata, T. Aida, Ferroelectric columnar liquid crystal featuring confined polar groups within core–shell architecture, Science 336 (2012) 209–213, doi:10.1126/science.1217954.

[68] Z. Chen, Y. Suzuki, A. Imayoshi, X. Ji, K.V. Rao, Y. Omata, D. Miyajima, E. Sato, A. Nihonyanagi, T. Aida, Solvent-free autocatalytic supramolecular polymerization, Nat. Mater. 21 (2022) 253–261, doi:10.1038/s41563-021-01122-z.

[69] Q. Xiao, T. Sakurai, T. Fukino, K. Akaike, Y. Honsho, A. Saeki, S. Seki, K. Kato, M. Takata, T. Aida, Propeller-shaped fused oligothiophenes: a remarkable effect of the topology of sulfur atoms on columnar stacking, J. Am. Chem. Soc. 135 (2013) 18268–18271, doi:10.1021/ja4092769.

[70] J. Kang, D. Miyajima, T. Mori, Y. Inoue, Y. Itoh, T. Aida, A rational strategy for the realization of chain-growth supramolecular polymerization, Science 347 (2015) 646–651, doi:10.1126/science.aaa4249.

[71] K. Venkata Rao, D. Miyajima, A. Nihonyanagi, T. Aida, Thermally bisignate supramolecular polymerization, Nat. Chem. 9 (2017) 1133–1139, doi:10.1038/nchem.2812.

[72] K. Yano, Y. Itoh, F. Araoka, G. Watanabe, T. Hikima, T. Aida, Nematic-to-columnar mesophase transition by in situ supramolecular polymerization, Science 363 (2019) 161–165, doi:10.1126/science.aan1019.

[73] T. Aida, E.W. Meijer, Supramolecular polymers – we've come full circle, Isr. J. Chem. 60 (2020) 33–47, doi:10.1002/ijch.201900165.

[74] M. Ueda, T. Aoki, T. Akiyama, T. Nakamuro, K. Yamashita, H. Yanagisawa, O. Nureki, M. Kikkawa, E. Nakamura, T. Aida, Y. Itoh, Alternating heterochiral supramolecular copolymerization, J. Am. Chem. Soc. 143 (2021) 5121–5126, doi:10.1021/jacs.1c00823.

[75] X.J. Zhang, D. Morishita, T. Aoki, Y. Itoh, K. Yano, F. Araoka, T. Aida, Anomalous Chiral transfer: supramolecular polymerization in a chiral medium of a mesogenic molecule, Chem. Asian J. 17 (2022) e202200223, doi:10.1002/asia.202200223.

[76] T. Aoki, M. Ueda, T. Aida, Y. Itoh, Supramolecular polymerization of a photo-fluttering chiral monomer: a temporarily suspendable chain growth by light, J. Am. Chem. Soc. 144 (2022) 7080–7084, doi:10.1021/jacs.2c02176.

[77] L. Su, J. Mosquera, M.F.J. Mabesoone, S.M.C. Schoenmakers, C. Muller, M.E.J. Vleugels, S. Dhiman, S. Wijker, A.R.A. Palmans, E.W. Meijer, Dilution-induced gel-sol-gel-sol transitions by competitive supramolecular pathways in water, Science 377 (2022) 213–218, doi:10.1126/science.abn3438.

[78] A.K. Mondal, M.D. Preuss, M.L. Śleczkowski, T.K. Das, G. Vantomme, E.W. Meijer, R. Naaman, Spin filtering in supramolecular polymers assembled from achiral monomers mediated by chiral solvents, J. Am. Chem. Soc. 143 (2021) 7189–7195, doi:10.1021/jacs.1c02983.

[79] M.L. Śleczkowski, M.F.J. Mabesoone, P. Śleczkowski, A.R.A. Palmans, E.W. Meijer, Competition between chiral solvents and chiral monomers in the helical bias of supramolecular polymers, Nat. Chem. 13 (2021) 200–207, doi:10.1038/s41557-020-00583-0.

[80] E. Weyandt, L. Leanza, R. Capelli, G.M. Pavan, G. Vantomme, E.W. Meijer, Controlling the length of porphyrin supramolecular polymers via coupled equilibria and dilution-induced supramolecular polymerization, Nat. Commun. 13 (2022) 248, doi:10.1038/s41467-021-27831-2.

[81] H. Su, S.A.H. Jansen, T. Schnitzer, E. Weyandt, A.T. Rösch, J. Liu, G. Vantomme, E.W. Meijer, Unraveling the complexity of supramolecular copolymerization dictated by triazine–benzene interactions, J. Am. Chem. Soc. 143 (2021) 17128–17135, doi:10.1021/jacs.1c07690.

[82] M.F.J. Mabesoone, A.R.A. Palmans, E.W. Meijer, Solute–solvent interactions in modern physical organic chemistry: supramolecular polymers as a muse, J. Am. Chem. Soc. 142 (2020) 19781–19798, doi:10.1021/jacs.0c09293.

[83] R.P.M. Lafleur, S. Herziger, S.M.C. Schoenmakers, A.D.A. Keizer, J. Jahzerah, B.N.S. Thota, L. Su, P.H.H. Bomans, N.A.J.M. Sommerdijk, A.R.A. Palmans, R. Haag, H. Friedrich, C. Böttcher, E.W. Meijer, Supramolecular double helices from small C_3-symmetrical molecules aggregated in water, J. Am. Chem. Soc. 142 (2020) 17644–17652, doi:10.1021/jacs.0c08179.

[84] P.K. Hashim, J. Bergueiro, E.W. Meijer, T. Aida, Supramolecular polymerization: a conceptual expansion for innovative materials, Prog. Polym. Sci. 105 (2020) 101250, doi:10.1016/j.progpolymsci.2020.101250.

[85] M. Peterca, M.R. Imam, A.E. Dulcey, K. Morimitsu, Q. Xiao, D.S. Maurya, V. Percec, Molecular parameters including fluorination program order during hierarchical helical self-organization of self-assembling dendrons, Giant 11 (2022) 100103, doi:10.1016/j.giant.2022.100103.

[86] D. Sahoo, M. Peterca, M.R. Imam, B.E. Partridge, Q. Xiao, V. Percec, Conformationally flexible dendronized cyclotetraveratrylenes (CTTV)s self-organize a large diversity of chiral columnar, Frank-Kasper and quasicrystal phases, Giant 10 (2022) 100096, doi:10.1016/j.giant.2022.100096.

[87] M.R. Imam, M. Peterca, Q. Xiao, V. Percec, Enhancing conformational flexibility of dendronized triphenylene via diethylene glycol linkers lowers transitions of helical columnar, Frank-Kasper, and quasicrystal phases, Giant 10 (2022) 100098, doi:10.1016/j.giant.2022.100098.